JCB Article

Overlapping functions of the cell adhesion molecules Nr-CAM and L1 in cerebellar granule cell development

Takeshi Sakurai,[1] Marc Lustig,[2] Joanne Babiarz,[1] Andrew J.W. Furley,[3] Steven Tait,[4] Peter J. Brophy,[4] Stephen A. Brown, [5] Lucia Y. Brown,[5] Carol A. Mason,[6] and Martin Grumet[1]

[1]W.M. Keck Center for Collaborative Neuroscience, Rutgers University, Piscataway, NJ 08854
[2]Department of Pharmacology, New York University Medical Center, New York, NY 10016
[3]Centre for Developmental Genetics, University of Sheffield, Sheffield S10 2TN, UK
[4]Department of Preclinical Veterinary Sciences, University of Edinburgh, Edinburgh EH8 9YL, UK
[5]Department of Obstetrics and Gynocology and [6]Department of Pathology, Anatomy and Cell Biology, and Center for Neurobiology and Behavior, Columbia University, College of Physicians and Surgeons, New York, NY 10032

The structurally related cell adhesion molecules L1 and Nr-CAM have overlapping expression patterns in cerebellar granule cells. Here we analyzed their involvement in granule cell development using mutant mice. Nr-CAM–deficient cerebellar granule cells failed to extend neurites in vitro on contactin, a known ligand for Nr-CAM expressed in the cerebellum, confirming that these mice are functionally null for Nr-CAM. In vivo, Nr-CAM–null cerebella did not exhibit obvious histological defects, although a mild size reduction of several lobes was observed, most notably lobes IV and V in the vermis. Mice deficient for both L1 and Nr-CAM exhibited severe cerebellar folial defects and a reduction in the thickness of the inner granule cell layer. Additionally, anti-L1 antibodies specifically disrupted survival and maintenance of Nr-CAM–deficient granule cells in cerebellar cultures treated with antibodies. The combined results indicate that Nr-CAM and L1 play a role in cerebellar granule cell development, and suggest that closely related molecules in the L1 family have overlapping functions.

Introduction

Cell adhesion molecules (CAMs)* mediate cell–cell interactions in both the developing and mature nervous system. CAMs of the immunoglobulin superfamily mediate several aspects of nervous system development including cell adhesion and migration, axonal growth, fasciculation, and guidance, as well as target recognition, synapse formation, and plasticity (Brummendorf and Rathjen, 1995; Schachner, 1997). The function of L1 has been shown to be particularly important, as mutations in the L1 gene in humans cause congenital developmental defects such as corpus callosum agenesis, mental retardation, adducted thumbs, spastic paraplegia, and hydrocephalus, known collectively as CRASH syndrome (Kamiguchi et al., 1998). L1 knockout mice serve as a useful model of this syndrome as they show phenotypic characteristics similar to this human brain malformation, including hydrocephalus, corpus callosum dysgenesis, and defects in the corticospinal tract due to errors in axon guidance (Dahme et al., 1997; Cohen et al., 1998; Fransen et al., 1998; Demyanenko et al., 1999; Rolf et al., 2001).

CAMs in the L1 family include L1, Nr-CAM, CHL1, and neurofascin, all of which have six Ig domains, 4/5 fibronectin type III repeats in their extracellular region, and a highly conserved cytoplasmic region (Grumet, 1997; Hortsch, 2000). Despite structural similarities to L1, Nr-CAM has a more restricted expression pattern (Lustig et al., 2001). Nr-CAM is expressed transiently in ventral midline structures in the developing brain, including the floor plate where it has been implicated in axonal guidance through interaction with a related CAM, TAG-1/axonin-1 (Stoeckli and Landmesser,

Address correspondence to Martin Grumet, W.M. Keck Center for Collaborative Neuroscience, Rutgers, State University of New Jersey, 604 Allison Rd., Piscataway, NJ 08854-8082. Tel.: (732) 445-6577. Fax: (732) 445-2063. E-mail: mgrumet@rci.rutgers.edu

T. Sakurai's present address is Mount Sinai School of Medicine, Department of Biochemistry and Molecular Biology and Neurology, New York, NY 10029.

*Abbreviations used in this paper: C, carbonic anhydrase; CAM, cell adhesion molecule; EGL, external granule cell layer; IGL, inner granule cell layer; RPTPβ, receptor protein tyrosine phosphatase β; S, spacer region.

Key words: cerebellum; Nr-CAM; L1; cell adhesion molecule; development

1995; Stoeckli et al., 1997; Lustig et al., 1999, 2001). In vitro, Nr-CAM induces neurite outgrowth from dorsal root ganglia neurons when it is presented as a substrate (Lustig et al., 1999). Nr-CAM also serves as a receptor for several neuronal recognition molecules, including contactin, neurofascin, and receptor tyrosine phosphatase β (RPTPβ) (Morales et al., 1993; Volkmer et al., 1996; Sakurai et al., 1997). These multiple binding partners may explain its purported diverse roles during nervous system development in several regions including the spinal cord, the visual system, and the cerebellum (Grumet et al., 1991; Kayyem et al., 1992; Krushel et al., 1993; Stoeckli and Landmesser, 1995; Lustig et al., 1999, 2001).

Cerebellar granule cells are a good model system for studying molecular and cellular developmental processes in the nervous system (Hatten and Heintz, 1995). Granule cells develop from the rhombic lip anlage and migrate to the surface of the prospective cerebellum. These cells proliferate rapidly, resulting in formation of the external granule cell layer (EGL), and then differentiate into postmitotic granule cells during the first two weeks after birth (Hatten et al., 1997; Alder et al., 1999). Granule cell proliferation is postulated to have a role in the formation of the cerebellar fissures and lobes (Mares and Lodin, 1970; Yang et al., 1999). In addition, interactions between granule cells and Purkinje cells are important for differentiation of both cells (Baptista et al., 1994; Morrison and Mason, 1998). The inward migration of postmitotic granule cells is marked by the expression of several proteins, including TAG-1 and L1 (Kuhar et al., 1993; Stottmann and Rivas, 1998). As they begin this migration, they extend L1 positive axons horizontally that form the parallel fibers in the molecular layer and their cell bodies continue to migrate and eventually form the inner granule cell layer (IGL) under the Purkinje cell layer. Antibody perturbation experiments indicated a role for L1 in granule cell migration in tissue explants (Lindner et al., 1983; Hoffman et al., 1986), but surprisingly, cerebella in L1-null mice are relatively normal (Fransen et al., 1998; Demyanenko et al., 1999), suggesting that other molecules, perhaps related CAMs, might compensate for absence of L1 function.

To investigate Nr-CAM function in the cerebellum in vivo, we prepared Nr-CAM–deficient mice by homologous recombination. Nr-CAM is expressed on both granule cells and Purkinje cells in developing chick (Krushel et al., 1993) and mouse (this study) cerebellum. Nr-CAM–deficient mice are viable and exhibit subtle size difference in lobes in the vermis of the cerebellum. Nevertheless, cerebellar granule neurons from these mice failed to respond in vitro to contactin substrates that induce neurite outgrowth from wild-type cells, confirming that these mice are functionally null for Nr-CAM. These results suggest the involvement of Nr-CAM in cerebellar cell development but its absence may be compensated by overlapping functions of other closely related CAMs such as L1. Consistent with this idea, cerebellar granule cells from Nr-CAM–null mice placed in culture were more sensitive to treatment with antibodies against L1 than the cells from wild-type mice. Functional overlap between Nr-CAM and L1 was further demonstrated by the observation that mice deficient for both Nr-CAM and L1 exhibit severe cerebellar folial defects and reduction in the thickness of the IGL.

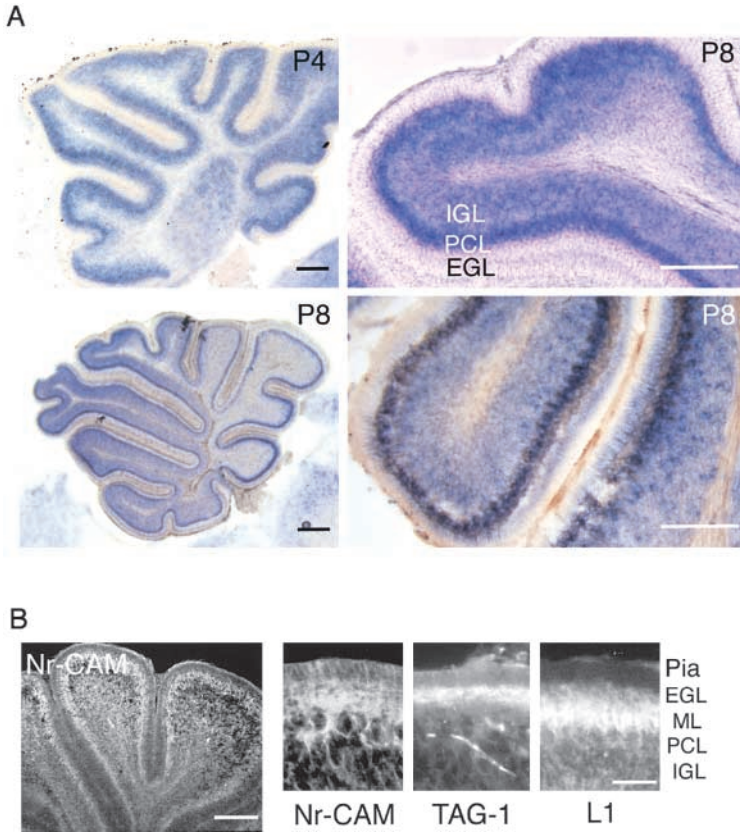

Figure 1. **Expression of Nr-CAM in mouse cerebellum.** (A) In situ hybridization on sagittal sections from P4 and P8 cerebellum was performed using an Nr-CAM specific probe. The bottom two panels are in situ hybridization followed by staining with anti-calbindin antibody with anti–mouse antibody-HRP and DAB reaction to visualize the Purkinje cell layer. Nr-CAM is expressed in the Purkinje cell layer (PCL) and IGL, but not in the EGL. Note in the bottom two panels that the Purkinje cell bodies are positive both for calbindin immunohistochemistry and for Nr-CAM by in situ hybridization. (B) Mid sagittal sections were prepared from P8 mouse cerebellum and stained with anti–Nr-CAM, anti-TAG-1, and anti-L1 antibodies. Nr-CAM is most robust in the molecular layer that is right below the TAG-1 positive inner EGL. Nr-CAM is also positive around Purkinje cells. L1 is positive in both the TAG-1 positive area and the molecular layer. Note that L1 is not expressed on Purkinje cells. Bars: (A, left bottom), 200 μm; (A, other panels), 100 μm; (B, left panel), 200 μm; (B, other panels), 50 μm.

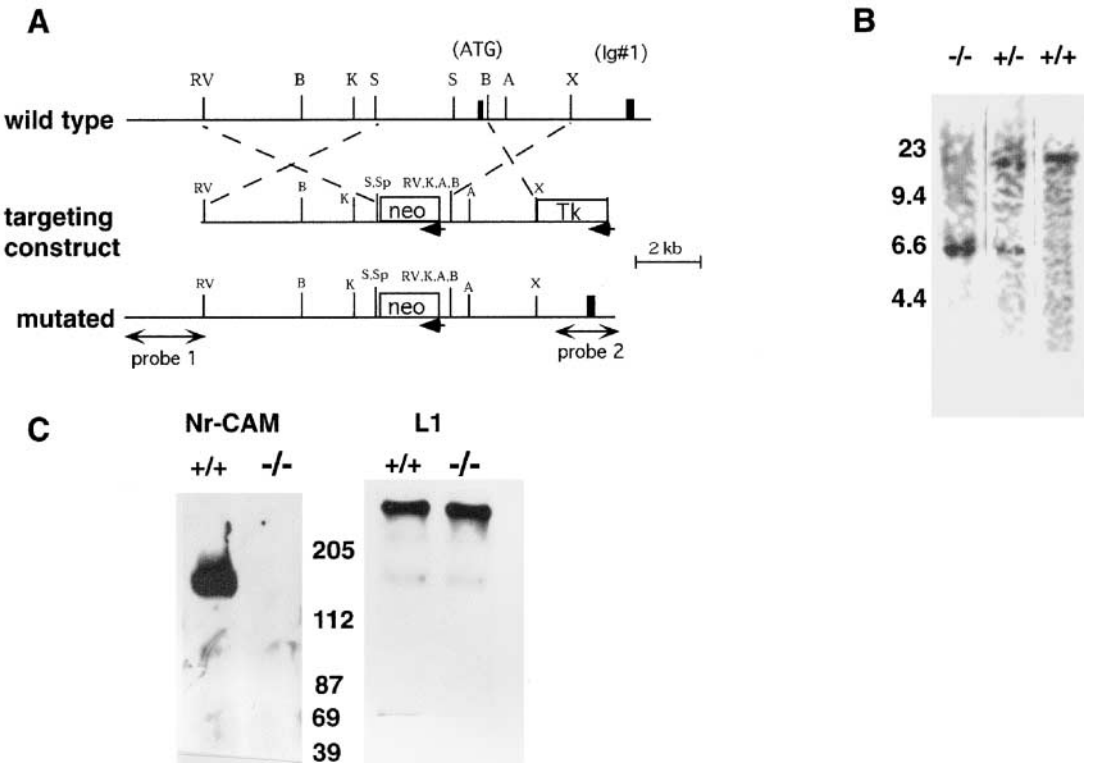

Figure 2. **Generation of Nr-CAM null mice.** (A) Genomic organization of Nr-CAM gene and gene targeting construct. One clone containing the region from the first intron to forth exon was obtained by genomic screening. The second exon, which encodes the initiation codon (ATG) and signal sequence for Nr-CAM (black box, middle), was replaced with a neo cassette. Direction of transcription for neo is opposite to that of Nr-CAM as indicated by arrow. The black box at the right end represents the fourth exon, which encodes half of first Ig domain (Ig #1). Probes 1 and 2 were used for screening of targeted embryonic stem cells. (B) Southern blot analysis of genomic DNAs from 4-wk-old progeny. DNA was extracted from tail and digested with EcoRV. Nonradioisotope Southern hybridization with probe 2 was performed as described in Materials and methods. Wild-type allele gives ~15-kbp band, whereas mutated allele gives ~6-kbp band. DNA standards in kbp are shown on the left side. (C) Western blot analysis of adult brain extracts. 20 μg of extract were subjected to 7% SDS PAGE and blotted with anti–Nr-CAM and anti-L1 antibodies. Anti–Nr-CAM antibody recognizes a 140-kD band which corresponds to cleaved Nr-CAM extracellular region. No bands were detected in the −/− extract. Anti-L1 antibody recognizes a 200-kD band and weak 140-kD band both in wild-type and −/− extracts. Molecular mass markers in kD are shown at their respective positions between the two panels.

Results

Nr-CAM is expressed on granule and Purkinje cells in developing mouse cerebellum

The expression pattern of Nr-CAM mRNA and protein was examined in the mouse cerebellum and compared with those of other CAMs. In situ hybridization showed that at postnatal day P4 and P8, Nr-CAM mRNA expression was most prominent in the Purkinje cell layer identified by calbindin immunostaining (Fig. 1 A). It was also detected in the IGL, and in the molecular layer directly superficial to Purkinje cells, but not in the EGL. Immunostaining with anti–Nr-CAM antibodies confirmed the expression of the protein on Purkinje cells and in the molecular layer at P8 (Fig. 1 B). The latter may reflect contributions both from Purkinje cell dendrites and granule cell axons. The closely related CAM, L1, has an overlapping distribution with Nr-CAM in the molecular layer, where it is expressed robustly on bundles of granule cell axons (Fig. 1 B). L1 is also expressed in the inner portion of the EGL, to a lesser extent than in the molecular layer. In contrast, TAG-1, a CAM that binds to Nr-CAM (Suter et al., 1995) and L1 (Buchstaller et al., 1996), is expressed transiently in the inner EGL on postmitotic granule cells (Fig. 1 B) (Kuhar et al., 1993). Thus, TAG-1 expression precedes that of L1 and Nr-CAM, and the latter two CAMs persist on granule cells in the IGL where TAG-1 expression is downregulated. Given the high degree of structural conservation between Nr-CAM and L1, the coexpression of these CAMs on granule cells raised the possibility of overlap in their functions on granule cells.

Generation of Nr-CAM–deficient mice

To investigate Nr-CAM function in the cerebellum in vivo, we prepared Nr-CAM knockout mice using homologous recombination (Fig. 2 A). The second exon was deleted to remove the ATG translation initiation codon and the signal sequence of Nr-CAM. Southern blotting using a 3′ probe distinguished between wild-type and mutated alleles (Fig. 2 B). Two independent mouse lines were established from two independent ES cell lines. Genomic Southern blotting analysis of 4-wk-old progeny revealed that the expected numbers of homozygotes following the Mendelian rule were obtained from matings between heterozygotes for the Nr-CAM mutation, suggesting that this mutation is not lethal. Homozygotes for the Nr-CAM mutation were viable at least up to 1.5 y and fertile. Western blotting using polyclonal anti–mouse Nr-CAM antibody did not detect any protein in

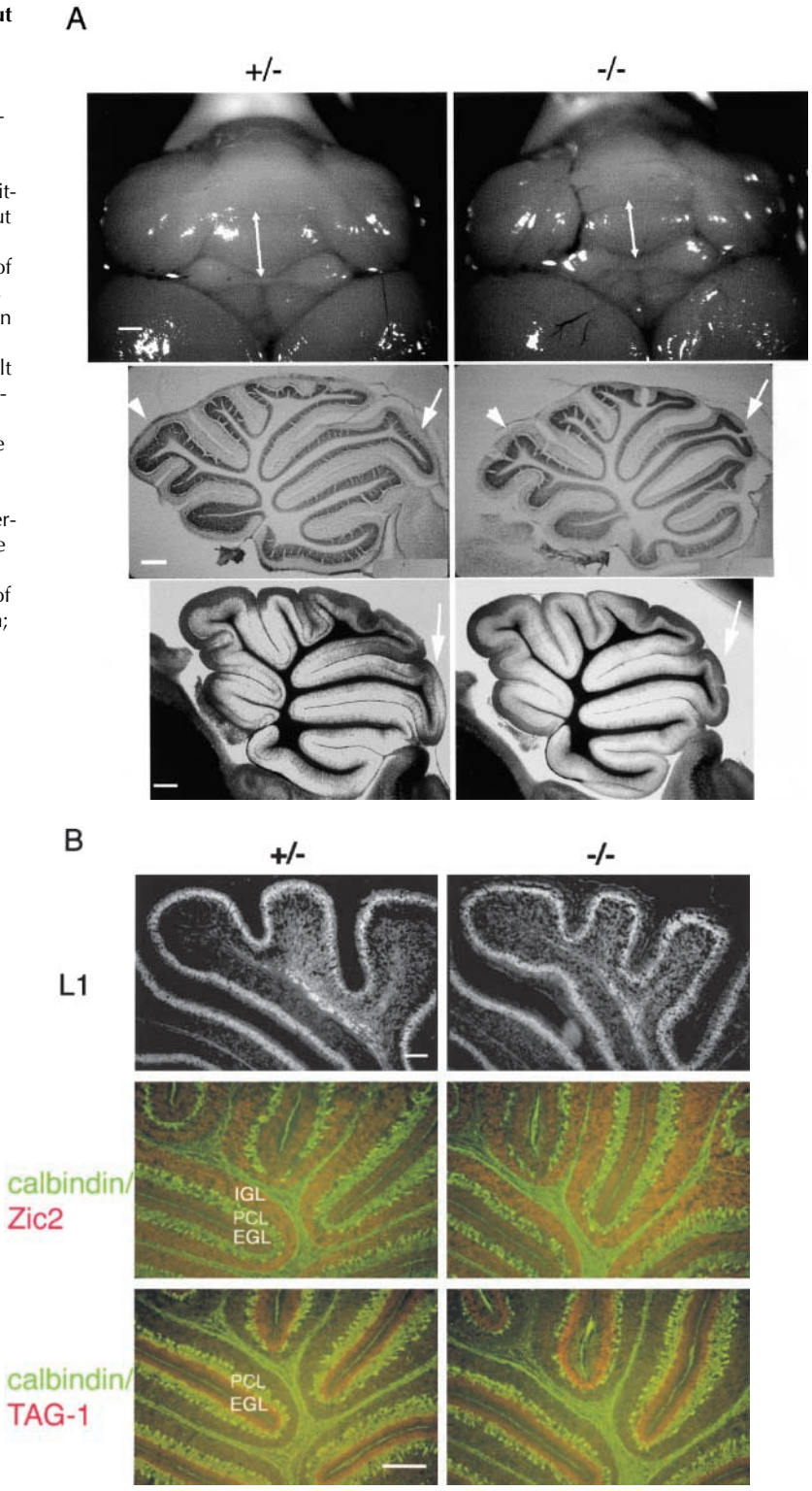

Figure 3. **Histological analysis of Nr-CAM knockout mouse cerebellum.** (A) (Top panels) Adult cerebella from Nr-CAM knockout mouse and its littermate heterozygote were observed under dissecting microscope and images were collected through CCD camera. Note that the length in anterior-posterior axis of lobes IV and V at the midline is shorter in Nr-CAM knockout mouse. (Middle panels) Vibratome midsagittal sections of cerebella from adult Nr-CAM knockout mouse and its littermate heterozygote were stained with cresyl violet. Note that lobes IV and V (arrows) of homozygotes are smaller than those of heterozygous littermates. In contrast, there was little or no change in the size of lobe IX (arrowheads). (Bottom panels) Vibratome midsagittal sections of cerebella from adult Nr-CAM knockout mouse and its littermate heterozygote were visualized under phase contrast microscope. (B) P8 cerebella from Nr-CAM knockout mice and its heterozygous littermates were cryosectioned sagittally and stained with antibodies against L1, calbindin, Zic2 and TAG-1. There is no obvious difference between heterozygotes and homozygotes. Note that the IGL is Zic2 positive, the Purkinje cell layer (PCL) is positive for calbindin, and the inner region of the EGL is positive for TAG-1. Bars: (A, top), 400 μm; (A, middle), 400 μm; (A, bottom), 400 μm; (B, top) 100 μm; (B, middle, bottom), 200 μm.

adult brain extracts from homozygotes (Fig. 2 C). In addition, immunostaining of brain sections from homozygotes did not show any signal with anti–Nr-CAM antibody (unpublished data), suggesting that these homozygotes are protein null for Nr-CAM. Homozygotes and heterozygotes were indistinguishable in terms of overall body size, activity, and growth rate (total >600 mice); this is in contrast to L1 null mice that we raised, which were visibly smaller than their littermates as described (Cohen et al., 1998).

Nr-CAM–deficient mouse cerebellum shows mild size reduction in specific lobes

Gross observation of whole mount adult cerebella revealed a slight difference in the size of lobes IV and V (Fig. 3 A). Analysis of sagittal sections of the brains confirmed a mild size reduction in specific lobes (i.e., IV and V) in the midsagittal region of Nr-CAM–deficient mouse cerebella, but otherwise there were no dramatic differences compared with wild type. When compared with littermate heterozygotes,

Table I. **Quantitation of size of cerebellar lobes**

	Percentage of area of Nr-CAM −/− compared to area of Nr-CAM +/−
lobe I + II	92.9 ± 0.4
lobe III	95.9 ± 2.3
lobe IV + V	88.7 ± 2.1
lobe VI	97.0 ± 0.9
lobe VII	104.8 ± 3.3
lobe IX	98.8 ± 0.7
lobe X	93.9 ± 1.1

Measurements were made on 2–3 vibratome sections (100 μm thickness) from cerebella of adult females (3–6 mo old, inbred genetic background, three pairs of +/− and −/−). Area of gray matter in each lobe (Fig. 3) was measured using NIH image. The percentage of the size of homozygotes compared to size of heterozygous littermate control was calculated, and average ± SD is shown.

the area of gray matter measured in sections of these lobes was 11% smaller in Nr-CAM–null mice than in littermate heterozygotes (Table I). This was due to a reduction in the length of the lobule, rather than to a reduction in the thickness of the molecular layer, which was similar in Nr-CAM–deficient mice and littermate heterozygotes (Fig. 3 A). In addition, lobes I and II, and lobe X are also slightly (6–7%) smaller than littermate controls.

Despite the expression of Nr-CAM in both granule and Purkinje cells, there was no obvious histological difference between adult cerebella of Nr-CAM–null, heterozygotes, and wild-type mice. We also analyzed P4 and P8 cerebella by staining with L1, neurofascin, TAG-1, Zic2 (unpublished data; Aruga et al., 1996; Dahmane and Ruiz-i-Altaba, 1999), and calbindin (Mason et al., 1990), but we did not detect any obvious differences with these histological markers compared with their littermate heterozygotes (Fig. 3 B and unpublished data). These results suggest that the absence of Nr-CAM resulted in only minor defects in particular folia with normal formation of the molecular and granule cell layers in the cerebellum.

Cerebellar cells from Nr-CAM–deficient mice fail to extend neurites in response to contactin

Because we did not observe obvious defects in the Nr-CAM–null mice in vivo, we asked if these mice are defective for Nr-CAM function using an in vitro neurite outgrowth assay. It has been shown that Nr-CAM binds to the neuronal CAM contactin, and serves as a receptor for contactin to induce neurite outgrowth from chick tectal cells (Morales et al., 1993). There is also evidence for an interaction between contactin expressed on CHO transfectants and Nr-CAM on mouse cerebellar neurons (Faivre-Sarrailh et al., 1999). Contactin has been shown to be expressed in the molecular layer (Berglund et al., 1999) where Nr-CAM is also expressed, and it is possible that interactions between these molecules occur in vivo.

When cerebellar cells isolated from wild-type P8 pups were plated onto a contactin–Fc substrate, we observed neurite outgrowth from these cells (Fig. 4 A). The degree of neurite outgrowth was comparable to that induced by chick L1 (Ng–CAM) (unpublished data) which is a potent promoter of neurite outgrowth (Lagenaur and Lemmon, 1987). Other substrates including Nr-CAM–Fc fusion protein or human Ig did not induce neurite outgrowth from the cerebellar cells (unpublished data). Contactin–Fc did not induce neurite outgrowth from dorsal root ganglia neurons prepared from embryonic day 14 mice (unpublished data), suggesting that the neurite outgrowth induced by contactin–Fc from cerebellar cells is cell-type specific. This contactin–Fc-induced neurite outgrowth was inhibited by the addition of anti–Nr-CAM Fab′ (Fig. 4 A). The anti–Nr-CAM antibody did not inhibit neurite outgrowth on L1 substrate, showing that this inhibition is substrate specific (unpublished data). These antibody perturbation studies suggest that cerebellar granule cells use Nr-CAM as a receptor for contactin to mediate neurite outgrowth.

When we plated cells from Nr-CAM–deficient mice, they did not extend neurites on the contactin-Fc substrate (Fig. 4 A), but they did extend neurites on an L1 substrate to the same extent as the wild-type cells (unpublished data). Therefore, the inability of the Nr-CAM–null cells to respond to contactin–Fc is substrate specific and not a result of cell preparation, e.g., cell viability. These results confirm that Nr-CAM functions as a receptor for contactin on cerebellar granule cells and suggest that our Nr-CAM knockout mice are indeed functionally null for Nr-CAM.

Cerebellar cells from Nr-CAM–deficient mice still extend neurites in response to RPTPβ

In addition to its function as a receptor for contactin, Nr-CAM can also serve as a coreceptor for RPTPβ to induce neurite outgrowth from chick tectal cells (Sakurai et al., 1997). In this case, Nr-CAM interacts with contactin on the same membrane forming a receptor complex for RPTPβ. Because contactin (Berglund et al., 1999), Nr-CAM (Fig. 1), and RPTPβ/phosphacan (soluble form of RPTPβ) (Grumet et al., 1994) are all expressed in the molecular layer of the cerebellum, we also analyzed RPTPβ-induced neurite outgrowth. When the βCFS–Fc fusion protein (an Fc fusion protein containing the extracellular region of RPTPβ, including carbonic anhydrase [C], fibronectin type III repeat [F], and spacer region [S] domains) (Sakurai et al., 1997), was used as a substrate, cerebellar cells extend neurites on this substrate (Fig. 4 B). This neurite outgrowth was inhibited by >40% with anti–Nr-CAM antibody treatment (Fig. 4 B), suggesting that Nr-CAM serves as a receptor (or at least one component of a receptor complex) for RPTPβ in mouse cerebellar granule cells. However, the neurite outgrowth from Nr-CAM deficient cells on RPTPβ was only marginally lower than that obtained from the wild-type cells (Fig. 4, B and C). Therefore, although Nr-CAM has been suggested to be involved in RPTPβ-induced neurite outgrowth, the ability of Nr-CAM–null cells to extend neurites on RPTPβ suggests that other molecules may compensate for Nr-CAM function.

To search for such molecules, we considered the known binding partners for RPTPβ, which binds to contactin through its C domain, and to Nr-CAM through its S domain (Sakurai et al., 1997). Contactin and Nr-CAM can form a complex that can bind to the C domain in RPTPβ even in the absence of the S domain (Sakurai et al., 1997). To analyze these interactions in mice, we examined proteins that were precipitated from mouse brain extract by βC–Fc fusion

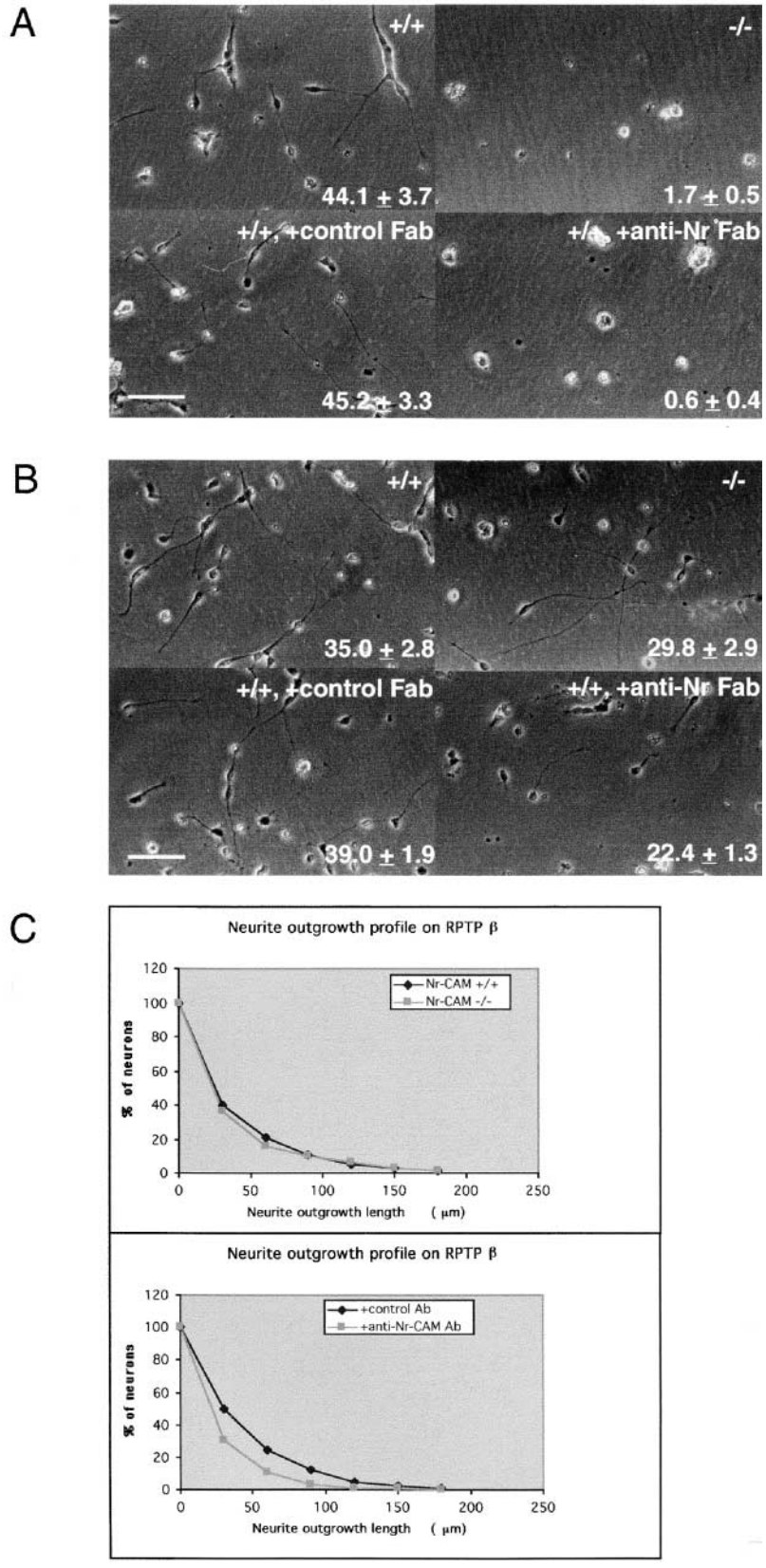

Figure 4. **Neurite outgrowth responses of cerebellar cells in vitro.** (A) Cerebellar cells from P8 wild type (+/+) and Nr-CAM$^{-/-}$ (−/−) mice (top panels) were plated on plastic dishes coated with contactin–Fc fusion protein (100 μg/ml) and incubated at 37°C. Note that cells prepared from −/− mice do not extend neurites on contactin–Fc substrate although they bound to the substrate. Bottom panels are cultures prepared from wild-type mice that were treated with Fab′ fragments of antibodies (100 μg/ml) against either Nr-CAM or plexin (control) by adding to the culture media 3 h after plating. Cultures were fixed 24 h later and photographs were taken. Neurite outgrowth lengths were measured as described using more than 100 cells for each condition. Numbers in each panel are averages of neurite outgrowth ± SD. Anti–Nr-CAM antibody treatment completely inhibited neurite outgrowth. (B) Cerebellar cells from P8 wild-type and Nr-CAM$^{-/-}$ (−/−) mice (top panels) were plated on plastic dishes coated with βCFS–Fc fusion protein (100 μg/ml) and incubated at 37°C. Bottom panels are cultures prepared from wild-type mice that were treated with Fab′ fragments of antibodies (100 μg/ml) against either Nr-CAM or plexin (control) by adding to the culture media 3 h after plating. Cultures were fixed 24 h later and photographs were taken. Neurite outgrowth lengths were quantitated as described using more than 100 cells for each condition. Numbers in each panel are averages of neurite outgrowth ± SD. Anti–Nr-CAM antibody treatment inhibited neurite outgrowth to ∼50% of control. In contrast, −/− cells extend neurites comparable to wild-type cells. (C) Neurite outgrowth plots of responses to RPTPβ. Percentages of neurons (vertical axis) with neurites longer than or equal to length indicated (horizontal axis) were plotted as described. Anti-Nr-CAM antibody treatment shifted profile to the left (bottom). Profile of neurite outgrowth from −/− cells is similar to that of wild-type cells (top). Bars: (A), 50 μm; (B) 50 μm.

protein that contains only the C domain. As shown in Fig. 5, βC–Fc precipitated contactin and Nr-CAM from wild-type mouse cerebellar extract. Because Nr-CAM does not bind directly to the C domain, its coprecipitation by βC–Fc must be in the form of a complex with contactin (Sakurai et al., 1997). As expected, βC–Fc did not precipitate Nr-CAM protein from Nr-CAM–deficient mouse brain extracts, but it did precipitate contactin in both cases (Fig. 5). Interestingly, antineurofascin antibody recognized a band at ∼150 kD in the βC–Fc precipitate from the Nr-CAM–deficient but not

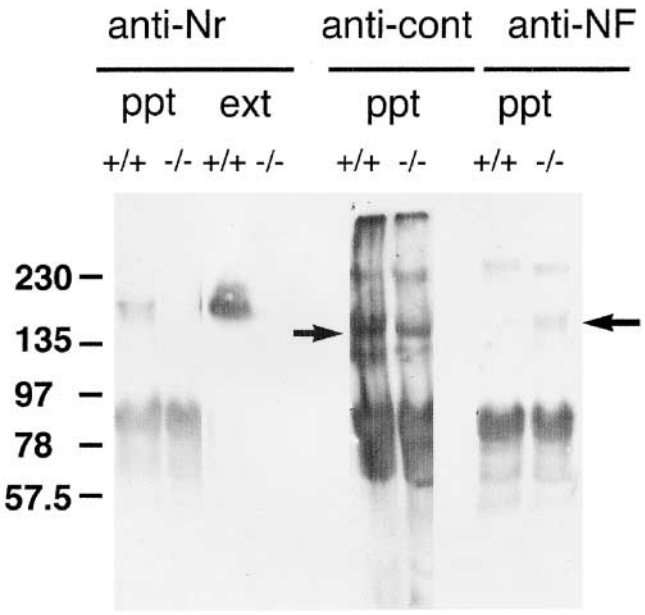

Figure 5. **Receptors for RPTPβ in wild-type and Nr-CAM–deficient brain.** P8 cerebellar extracts from wild type (+/+) or Nr-CAM–null (−/−) mice were incubated overnight with protein A beads that had been preincubated with βC–Fc fusion protein at 4°C and proteins bound to the beads were subjected to 7% SDS PAGE (ppt lanes). 20 μg of extracts were loaded in ext lanes. Western blotting was performed using anti–Nr-CAM, anti-contactin and antineurofascin antibodies. Nr-CAM was detected in precipitates with βC–Fc fusion protein from wild-type extract, but not from −/− extract. Contactin was precipitated by βC–Fc from both wild-type and −/− extracts as described previously (arrow in middle panel). Note that neurofascin is detected in the βC–Fc precipitate from −/− extract, but not from wild-type (arrow in right panel). Other bands that appeared in contactin and neurofascin blots are nonspecific and they include Igs that are recognized by secondary antibodies. Molecular weight markers in kD are shown at the left.

from the wild-type extract (Fig. 5). These results suggest that neurofascin, which has been found to bind to contactin, might replace Nr-CAM in Nr-CAM–deficient mice.

Mice deficient for both Nr-CAM and L1 have severe cerebellar defects

Given that neurofascin might be able to compensate for Nr-CAM function as a coreceptor for RPTPβ, we speculated that the reason why we did not detect dramatic defects in Nr-CAM knockout mice in vivo might be because of compensation by other members of L1 family CAMs (i.e., L1, neurofascin, and CHL1) for the loss of Nr-CAM. We considered these CAMs because they share highly conserved cytoplasmic regions that link to common cytoplasmic targets including ankyrin (Davis and Bennett, 1994). Moreover, L1 and possibly CHL1 expression patterns overlap with the Nr-CAM expression pattern, (i.e., on granule cells during critical stages of their development). Among these candidates, only L1 knockout mice have been reported, and these mice are viable despite the existence of several defects in the development of the nervous system (Dahme et al., 1997; Cohen et al., 1998; Fransen et al., 1998; Demyanenko et al., 1999) including a mild cerebellar defect (Fransen et al., 1998). We obtained the L1 knockout mice developed by Dr. P. Soriano (Fred Hutchinson Research Center, Seattle, WA) and maintained them in our animal facility. These mice showed a phenotype similar to that reported by Cohen et al. (1998) and Fransen et al. (1998), including body weight reduction (~30% compared with their littermates), sunken eyeballs, and male hemizygous sterility (Cohen et al., 1998; Fransen et al., 1998). The frequency of L1-null adult males in our colony was 15.6% (n = 5 out of 32 total mice), which is similar to the frequency observed in the mice kept elsewhere (Cohen et al., 1998) (currently 14.0%; n = 88 out of 629 total mice) on the same 129SvEv genetic background. Because the L1 gene is on the X chromosome and L1 hemizygous ($L1^{-/y}$) male mice are effectively sterile, we mated Nr-CAM–deficient ($Nr^{-/-}L1^{+/y}$) males and Nr-CAM heterozygous/L1 heterozygous ($Nr^{+/-}L1^{+/y}$) females. We noticed an increased rate of postnatal death in progeny from these matings, especially during the first 1–2 wk after birth. At the age of 3 wk when genotyping was routinely performed, there was deviation from the Mendelian proportions as shown in Table II. We observed reduced numbers of pups that were Nr-CAM homozygous/L1 heterozygous ($Nr^{-/-}L1^{+/-}$) females, and Nr-CAM heterozygous/L1 hemizygous ($Nr^{+/-}L1^{-/y}$) males. The frequency of L1-null males at 3 wk postnatal was 35.7% in Nr-CAM wild-type background (5 out of 14 males), whereas this frequency dropped to 9.4% in the Nr-CAM–deficient background (3 out of 32 males; Table II). Moreover, we did not detect any Nr-CAM homozygous/L1 hemizygous ($Nr^{-/-}L1^{-/y}$) males at 3 wk postnatally.

Table II. **Genotype of progenies from matings with Nr-CAM −/−, L1 +/y males and Nr-Cam +/−, L1+/− females**

	Genotype		No. of pups at age of 3 wk	Percent
	Nr	L1		
Male	+/−	+/y	20	23.0
	+/−	−/y	3	3.4
	−/−	+/y	9	10.3
	−/−	−/y	0	0
Female	+/−	+/+	13	14.9
	+/−	+/−	18	20.7
	−/−	+/+	19	21.8
	−/−	+/−	5	5.7

Pups from matings with Nr-CAM −/− males and Nr-CAM +/−, L1 +/− females were genotyped at age of 3 wk postnatal. Total of 87 pups from 13 litters was analyzed. Normal Mendelian segregation should give a probability of 12.5% for each genotype.

Within these litters we noticed that there were certain pups whose body weights were 40–70% (average ~60%) of their littermates at P3–P6. Genotyping of these pups when they could be recovered alive showed that they were Nr-CAM homozygous/L1 hemizygous ($Nr^{-/-}L1^{-/y}$) males. Moreover, these mice were never recovered alive later than P8. Gross anatomical analysis showed dramatic cerebellar dysgenesis in the Nr-CAM/L1-deficient mice (Fig. 6 A). Cerebellar lobes and fissures were less well developed compared with littermates of the same age. Although we also observed size reductions in other areas of the brain (Fig. 6 B; Table III), the reduction in cerebellar size was markedly greater (Table III). In addition, histological analysis of cerebella showed that the thickness of the IGL is reduced in double knockout mice while the thickness of EGL is relatively normal (Fig. 6 A). Quantitation of the thickness of EGL and IGL supports this observation (Table IV); whereas the reduction in the EGL in

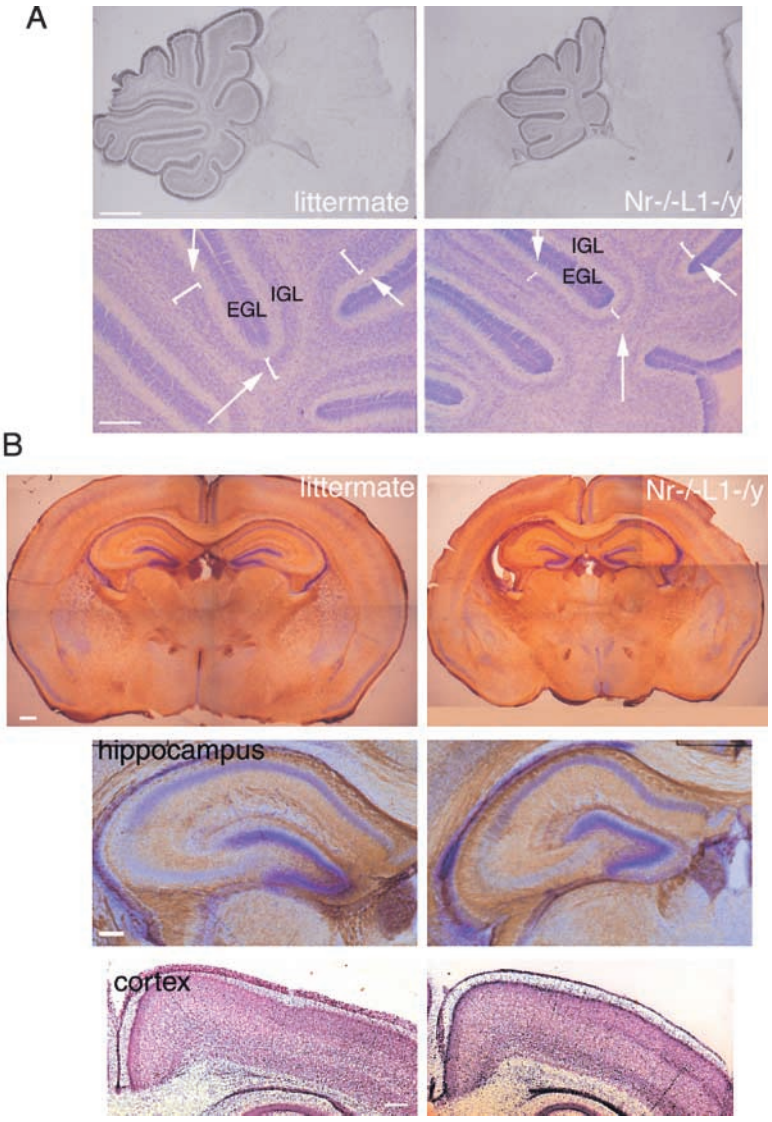

Figure 6. **Analysis of Nr-CAM/L1 double knockout brain.** (A) Vibratome sections were prepared from cerebella of Nr-CAM/L1 double knockout mouse and its littermate. Top panels are P6 cerebella stained with cresyl violet. Some fissures are missing or less well developed in double knockout mice compared with their littermates. Note that although the size of cerebellum is smaller in double knockout mouse, the size of brain stem is similar to that of littermate controls. Bottom panels are magnified views of top panels. Note that in comparable regions within the folia, the IGL is thinner in the double knockout than in the littermate control (arrows). Bars, 640 μm (top) and 160 μm (bottom). (B) Frontal vibratome sections were prepared from brain of double knockout mouse and its littermate at P5. Top and middle panels were stained with antineurofilament antibody following Nissl staining. Magnified views of hippocampal regions of top panels are shown in the middle panels. Although brain size is smaller, overall structures including hippocampus are similar between double knockout mouse and their littermate. Bottom panels show layer formation in cortex of double knockout mouse and its littermate visualized by Nissl staining on vibratome sections. Layer formation in cortex appears normal in double knockout mice. Bars: (top) 400 μm; (others) 200 μm.

Nr-CAM/L1 double knockout mice is 10–30%, the reduction in the IGL is 40–50% compared with their littermates. In contrast, in the cortex and hippocampus, layer formation appears normal in double knockout mice (Fig. 6 B).

To analyze which developmental stages are disrupted in Nr-CAM/L1 double knockout mouse cerebella, we performed immunostaining with markers for granule cell development. Staining for TAG-1 confirmed major defects in foliation and the thickness of the TAG-1 positive band may be reduced slightly (Fig. 7). However, TAG-1 was expressed appropriately in the inner EGL reflecting its normal temporal and spatial expression pattern on granule cells (Kuhar et al., 1993). In contrast, labeling for the transcription factor Zic2 (Aruga et al., 1996) that is normally expressed in the IGL was disrupted significantly in the double knockout mice (Fig. 7). The overall intensity of the Zic2 staining was diminished in the double mutants with many fewer Zic2-positive cells accumulating in the IGL. In some cases, more Zic2-positive cells were observed

Table III. **Analysis of brain size of Nr-CAM/L1 double knockout mice**

	Cerebellum	Cortex
P3–P4	71.2 ± 5.1%	96.2 ± 2.2%
P5–P6	56.3 ± 2.8%	85.2 ± 1.8%

Midsagittal sections of cerebella and frontal sections of cortex were used for analysis as described in Materials and methods. Area of sections from double knockout mice was compared to those of sections from littermates and the percentages of area are calculated. Numbers are average + SD (n = 3).

Table IV. **Measurement of thickness of EGL and IGL of Nr-CAM/L1 double knockout mice and their littermates**

	Layer	Lobe V	Lobe IX
Nr-CAM 1/1, L1−/y[a]	EGL	42.5 ± 2.3 (70.6%)	31.6 ± 3.2 (90.8%)
	IGL	30.8 ± 3.0 (51.0%)	35.6 ± 4.8 (58.9%)
Littermates[a]	EGL	64.0 ± 3.2 (100%)	34.8 ± 2.6 (100%)
	IGL	60.4 ± 2.1 (100%)	60.4 ± 3.0 (100%)

Cerebellar midsagittal sections from P5–P6 Nr-CAM/L1 double knockout mice and their littermates were processed for Nissl staining and images were captured by CCD camera. Thickness of EGL and IGL were measured in lobe V and IX using NIH image. Numbers are average + SD μm. Numbers in parentheses are the percentage of littermate control.
[a]n = 6.

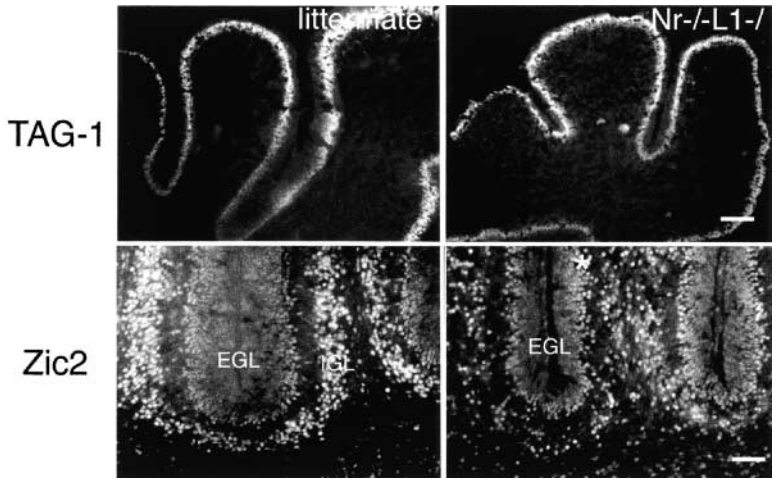

Figure 7. **Analysis of Nr-CAM/L1 double knockout mice cerebella.** Cryosections were prepared from cerebella of Nr-CAM/L1 double knockout mice and their littermates at P5. Sections were stained with anti-TAG-1 (top) and anti-Zic2 (bottom) antibodies. Note that although folial formation defect is obvious in TAG-1 staining, the expression pattern and level of TAG-1 are comparable to those of their littermate controls. In contrast, fewer Zic2-positive cells were found in the IGL in Nr-CAM/L1 double knockout mouse cerebella. In some regions in double knockout mice, Zic-2 positive cells are found below the EGL (*) rather than in the IGL. Bars, 100 μm (top), 50 μm (bottom).

right below the EGL rather than in their normal location in the IGL as seen in littermate controls (Fig. 7). These results suggest that the involvement of Nr-CAM and L1 in later stages of cerebellar granule cell development and the absence of both CAMs results in severe cerebellar developmental defects.

Anti-L1 antibody treatment perturbed maintenance of granule cells and their processes in cerebellar cultures from Nr-CAM knockout mice

Analysis of the Nr-CAM/L1 double knockouts suggested defects in granule cells during cerebellar development. To further test the involvement of Nr-CAM and L1 in granule cell development, we used a dissociated cerebellar culture that mimics the in vivo differentiation of granule and Purkinje cells (Hatten et al., 1998). As the double mutant mice were extremely difficult to obtain, we prepared mixed cerebellar cell cultures from mice deficient only for Nr-CAM and treated these cells with anti-L1 antibody to perturb L1 function in the absence of Nr-CAM. When Nr-CAM–deficient cultures were treated with control antibodies, granule cells developed extensive processes that are positive for α-internexin (Chien et al., 1996) (Fig. 8). At days and 11, anti-L1

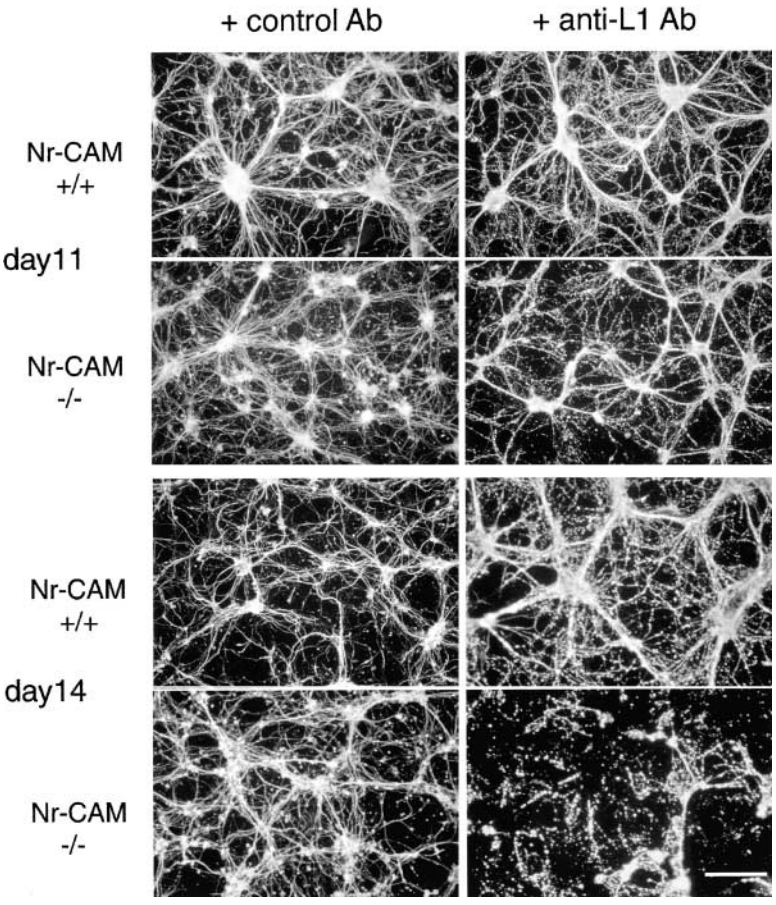

Figure 8. **Effects of perturbation of Nr-CAM and L1 in cerebellar culture in vitro.** Mixed cerebellar cultures were prepared from wild-type and Nr-CAM knockout mice and treated with anti-L1 antibody or control antibody (50 μg/ml). Cultures were fixed at d 11 and d 14, and stained with anti–α-internexin. Bar, 100 μm.

Table V. **Cell numbers in mixed cerebellar cultures treated with anti-L1 antibodies**

	Nr-CAM +/+	Nr-CAM −/−
Day 6	92.0%	98.5%
Day 11	64.3%	65.5%
Day 14	61.7%	23.2%

Cerebellar mixed cultures were prepared from wild-type or Nr-CAM knockout mice and after 3 d were treated with control or anti-L1 antibodies. Cultures were fixed at several time points and stained with Hoechst 33258. Numbers of nuclei were counted in two randomly chosen fields and these numbers were combined (range between ~500 and ~5000 nuclei). The percentage of cell numbers of culture treated with anti-L1 antibody compared to those of control antibody was calculated.

antibody treated cultures looked similar to control antibody treated cultures with an extensive meshwork of granule cell processes (Fig. 8). Nuclear staining showed that at d 6, similar numbers of cells were maintained in both control and anti-L1 antibody treated cultures prepared from wild-type and Nr-CAM–null mice (Table V). At d 11, however, we did see reduction in cell numbers in anti-L1 antibody treated cultures, although extensive processes were still observed. This reduction was observed in cultures prepared both from wild-type and Nr-CAM–null mice to a similar extent (~65% of control treated). At d 14, cell numbers in anti-L1 antibody treated culture from Nr-CAM–null mice dropped dramatically to 23.3% of control antibody treated cultures (Table V). Moreover, anti-L1 antibody treated cultures prepared from Nr-CAM–deficient mice had many fewer processes (Fig. 8). Cultures prepared from wild-type mice that were treated with anti-L1-antibody did not change dramatically between d 11 and 14 in terms of cell numbers surviving (~62% vs. 65% of control), and process formation (Fig. 8). The similarity in the morphology and numbers of cells in the cultures up to 11 d does not indicate any defects in cell adhesion to other cells or to the substrata. Rather, these data suggest that a lack of Nr-CAM disrupts survival and maintenance of granule cells and their neurites in the presence of function blocking anti-L1 antibodies at late stages in vitro (i.e., between day 11 and 14), and further support the notion that Nr-CAM and L1 have overlapping functions in granule cells.

Discussion

After cerebellar granule cells become postmitotic, they express L1 and Nr-CAM as they proceed to migrate and develop further. To analyze the function of Nr-CAM in cerebellar development, Nr-CAM–deficient mice were generated by homologous recombination. We did not detect Nr-CAM protein in brain extracts from these mice or by immunostaining of cryosections, verifying that they are Nr-CAM protein null. The mice are viable and fertile, and grow normally. Gross anatomical analysis of Nr-CAM null mice revealed only subtle defects in cerebellar folial formation, despite complete loss of granule cell response to contactin in culture. This might be explained by compensation by other CAMs with similar or overlapping functions with Nr-CAM. We found evidence that both neurofascin and L1 may compensate for the absence of Nr-CAM. In Nr-CAM–deficient cerebellar cells, neurofascin was found to coprecipitate with RPTPβ, normally a ligand of Nr-CAM. Moreover, a role for the closely related CAM, L1, is supported by our observations that Nr-CAM/L1 double knockout mice have severe cerebellar dysgenesis and that anti-L1 antibodies disrupts survival and maintenance of outgrowth of Nr-CAM–null granule cells in culture. These data suggest that L1 family CAMs are important for cerebellar granule cell development where their expression and functions appear to overlap.

Subtle phenotype in Nr-CAM–deficient mouse cerebellum

Nr-CAM is expressed on Purkinje and granule cells both in chick (Krushel et al., 1993) and in mouse cerebellum (Fig. 1). Based on the defects observed in neurite outgrowth for Nr-CAM mutant granule cells in vitro, we expected to find defects in cerebellar development of Nr-CAM–deficient mice in vivo. Although gross defects were not obvious by light microscopic analysis of the cerebellum, some lobes (i.e., IV and V in particular) in the vermis region are smaller than in heterozygous littermate controls. It has been postulated that granule cell proliferation plays a role in formation of the cerebellar fissures and lobes (Mares and Lodin, 1970). Overexpression of transcription factor Zipro1 in mouse cerebellum results in increased granule cell proliferation and affects the intralobular fissure formation (Yang et al., 1999). In Nr-CAM knockout mice, it seems that granule cell numbers are slightly decreased in particular lobes such as lobes IV and V, resulting in a reduction of the length of the lobe. However, Nr-CAM deficiency does not seem to affect the thickness of the granule cell layer. Nevertheless, it is possible that the formation of smaller folia in Nr-CAM knockout mice results from defects in development of cerebellar granule cells in vivo.

L1 knockout mice also have mild vermis hypoplasia that is seen in a different lobe (lobe VI) to the lobes most affected in Nr-CAM–null mice; in both cases a reduction of the length of the lobe was observed (Fransen et al., 1998). It is not clear why the defects that were detected in each of these single mutant animals are localized to a specific subset of lobes in the cerebellum. There is no evidence that any of the L1-like CAMs are variably expressed in these specific lobes. However, there is some evidence for regionalization of expression of the contactin-like molecules, some of which are known to interact with L1-like CAMs (Brummendorf and Rathjen, 1995). For example, BIG-2 is more highly expressed in anterior regions of the cerebellum (Yoshihara et al., 1995). As mutants in more of these molecules become available, further mutant combinations may also reveal whether these differences contribute to the regionalization in the cerebellum.

In view of similarities between the structure of L1 and Nr-CAM and their patterns of expression in the cerebellum, we produced Nr-CAM/L1 double knockout mice to further explore the function of L1 CAMs in cerebellar development.

Severe cerebellar defects in mice deficient for both Nr-CAM and L1

When we analyzed genotype of progeny from matings with $Nr^{-/-}L1^{+/y}$ males and $Nr^{+/-}L1^{+/-}$females in attempts to obtain Nr-CAM/L1 double knockout mice, we saw deviations of frequency from the predicted Mendelian results: there were decreased numbers of $Nr^{+/-}L1^{-/y}$ males and

$Nr^{-/-}L1^{+/-}$females, and no surviving $Nr^{-/-}L1^{-/y}$ males at 3 wk postnatally. We also set up matings with $Nr^{-/-}L1^{+/y}$ males and $Nr^{-/-}L1^{+/-}$ females, but so far we did not obtain any double knockout mice alive at 3 wk (unpublished data). Mice deficient for both Nr-CAM and L1 were smaller than their littermates and died by P8. Gross anatomical analysis revealed size reduction of brains, which is not surprising based on their body size reduction but they have more drastic size reduction of cerebella as well as underdevelopment of cerebella histologically (Table III).

It is clear that the cerebellar defect in the double knockout mice is more than just the sum of the L1 and the Nr-CAM single knockout phenotypes, as much more than just lobes IV and V plus lobe VI are affected. Other lobes are less well developed compared with their littermates, which is especially obvious in lobe IX (Fig. 6). In addition, the thickness of the IGL at P5–P6 is also decreased in the double mutant (Table IV), which is not observed in L1 or Nr-CAM single knockout mice. However, we could not exclude the possibility that this cerebellar dysgenesis reflects delayed development because we never recovered live double knockout mice at later than P8. Nevertheless, given that both Nr-CAM and L1 are expressed in granule cells and that the thickness of the IGL is reduced in double knockout mice, the severe cerebellar dysgenesis in double knockout mice seems most likely attributed to defects in granule cells. This idea is also supported by results that perturbation of both of these CAMs simultaneously in culture disrupts maintenance of granule cells (Fig. 8).

Granule cell development and L1 CAMs

How do mutations in L1-CAMs affect granule cell development? When granule cells become postmitotic, they first express TAG-1, and then L1 and Nr-CAM (Kuhar et al., 1993; Lindner et al., 1983 and this study). L1 and Nr-CAM subsequently become concentrated on their parallel fibers in the molecular layer but not TAG-1, which is not expressed in mature granule cells in the IGL. As granule cell bodies migrate towards the IGL, the transcription factor Zic-2 is turned on and serves as a later markers of granule cells during their migration (Fig. 3 B). In mice deficient for both Nr-CAM and L1, TAG-1 expression commences in the inner EGL and appears to be relatively normal, suggesting that even in the absence of Nr-CAM and L1, granule cells can go through this early stage. In contrast, the reduction of thickness of the IGL and the disruption in the pattern of Zic2 in the double knockouts suggest a role for these CAMs in later stages of granule cell differentiation as their cell bodies migrate from the EGL to the IGL. In culture, when both Nr-CAM and L1 functions were perturbed for 14 d, granule cell numbers decreased and the remaining granule cells lost most of their processes. These cultures appeared similar to control cultures at d 11 in vitro, suggesting that not adhesion per se but subsequent events necessary for maintaining granule cells and their neurites were affected when both Nr-CAM and L1 functions were perturbed.

Several possible mechanisms that are not mutually exclusive could explain the reduction of IGL formation and the loss of Zic2 expression in the IGL of the double knockouts. First, there may be an inhibition of granule cell proliferation in the EGL in the double mutants. However, given the robust expression of TAG-1, it seems that reasonable numbers of granule cells are produced and can undergo at least early stages of differentiation. Measurement of the thickness of the layers shows that reduction of thickness of EGL is not as severe as reduction of the IGL (Table IV). Second, induction of Zic2 expression may be inhibited or delayed. However, we were able to detect Zic2 expression 3–6 d after culturing Nr-CAM–null cerebellar cells in the presence of L1 antibodies, suggesting that the expression of Zic2 may not be inhibited even when both Nr-CAM and L1 are perturbed (unpublished data). In addition, we found some robust Zic2 positive cells in the IGL but in reduced numbers by comparison to littermate controls. Therefore, it seems that Zic2 expression may not be inhibited, but we can not exclude the possibility that Zic2 expression may be delayed in the double mutants. Third, granule cells may differentiate to express Zic2 but their migration may be impaired. Interestingly, there is evidence that disruption of parallel fiber extension can result in failure of granule cell migration (Tomoda et al., 1999). Given that both Nr-CAM and L1 are concentrated on their parallel fibers in the molecular layer in vivo and perturbation of both Nr-CAM and L1 causes loss of neurite extension in vitro, granule cell axon extension might also be affected in double knockout mice, resulting in migration defects of granule cells. It is also possible that these CAMs might directly be involved in granule cell migration. In any case, one might expect that such defects may result in ectopic accumulation of granule cells, for example, at the junction between the EGL and molecular layer. However, we did not observe massive accumulation of the cells at the junction although in some cases, there are more Zic-2 positive cells below the EGL than in the IGL (Fig. 7). This may be explained by the fourth possibility, that there may be increased granule cell death. It has been shown that L1 and CHL1 support survival of neurons in vitro (Chen et al., 1999). In fact, we observed a decrease of cell numbers in anti-L1 treated cultures at d 11 and d 14 even in wild type, and at d 14, cell numbers were reduced drastically in anti-L1 treated cultures prepared from Nr-CAM–deficient mice compared with wild-type cultures. Therefore, it is conceivable that L1 CAMs play a role in supporting granule cell survival. Among these possibilities, we favor a combination of the third and fourth possibilities. Whereas additional analyses of Nr-CAM/L1 double knockout mice may clarify the mechanism further, our data indicate that mutations in L1 CAMs most likely affects cerebellar granule cell development.

Although the reason why these mice die postnatally is not yet clear, the severity of the cerebellar dysgenesis may be sufficient to cause problems in motor coordination that compromise the ability of these mice to compete with their littermates in drinking sufficient amounts of milk.

Overlapping functions among L1 family CAMs

In contrast to the four known members of the L1 family in vertebrates, the neuroglian gene is known to represent a single homologue of the L1 family in *Drosophila* and gene duplication events during vertebrate evolution appear to have generated several L1-like CAMs (Hortsch, 2000). Although

these CAMs have clearly diverged in some of their functions and domains of expression, their basic structures and functions appear to have been conserved and substantial domains of their expression remain overlapping. Accordingly, the removal of just one member of the family may not result in a dramatic phenotype, as is born out by ours and previous analyses of the L1 single knockout phenotypes (Dahme et al., 1997; Cohen et al., 1998; Demyanenko et al., 1999). However, as we showed here, removal of both L1 and Nr-CAM results in severe disruption, particularly in the cerebellum where the molecules are normally coexpressed in granule cells. There are two possible interpretations of this result. One is that L1 and Nr-CAM share overlapping functions such that the absence of one molecule can be compensated substantially by the other molecule, but that removal of both molecules results in more severe defects. The other possibility is that L1 and Nr-CAM function independently but the absence of both has cumulative effects, resulting in much more deleterious phenotypes. Although we can not exclude the latter possibility completely, we favor the former for the following reasons. First, as noted above, cerebellar dysgenesis in Nr-CAM/L1 double knockout mice is not just the sum of two different phenotypes: for example, neither of the single knockout mice have reduction of IGL thickness. Second, although Nr-CAM and L1 are distinct CAMs, they bind to common ligands including TAG-1, contactin, RPTPβ/phosphacan, and laminin that are expressed in the cerebellum (Brummendorf and Rathjen, 1995; Grumet, 1997). Third, Nr-CAM and L1 have very similar cytoplasmic regions, which contain binding sites for ankyrin (Davis and Bennett, 1994). In addition, they have similar sequences, which are tyrosine phosphorylated in vivo during development (Garver et al., 1997; Tuvia et al., 1997). Therefore, it is conceivable that Nr-CAM and L1 share similar downstream targets to transmit transmembrane signals to regulate the cytoskeleton. In fact, ankyrinB knockout mice have been shown to have similar phenotype to L1 knockout mice (Scotland et al., 1998), suggesting that L1 and ankyrinB are on the same pathway. Moreover, while this manuscript was in preparation, it was group reported that knockout mice for Nr-CAM as well as ankyrinB both showed cataracts, suggesting that interactions between these proteins is important for lens development where both molecules are expressed (More et al., 2001). It is possible that both Nr-CAM and L1 use ankyrinB as a common down stream molecule in cerebellar granule cells.

We also found that in the absence of Nr-CAM, the related CAM neurofascin may replace Nr-CAM in a complex that interacts with RPTPβ (Fig. 5). This result suggests that Nr-CAM may also have overlapping functions with the other related CAMs such as CHL1 and neurofascin where they are co-expressed, such as cerebellum (Holm et al., 1996, and this study).

Concluding remarks

The results provide the first genetic evidence for potential overlapping functions between Nr-CAM and L1 and predict genetic interactions with other members of this family (i.e., neurofascin and CHL1). The notion that members of this family have similar or overlapping functions provides possible explanation for why many of the functions proposed for these CAMs on the basis of tissue and cell culture assays in vertebrates may not be reflected when only one member is deleted in knockout mice (for review see Brummendorf and Rathjen, 1995; Hortsch, 2000). Therefore, it will be informative to analyze various types of mutations in L1 family members in different combinations including genetically deficient mice and CAM mutants including overexpression and misexpression.

Materials and methods

Generation of Nr-CAM–null mice

Mouse Nr-CAM cDNA clones, which cover the entire Nr-CAM coding sequence, were cloned from λgt11 mouse embryo library (CLONTECH Laboratories, Inc.), and RNA was prepared from P8 mouse brains, using chick Nr-CAM full-length cDNA as a probe. The DNA sequence is highly homologous to the sequences reported for rat, human and chick Nr-CAM (Grumet et al., 1991; Kayyem et al., 1992; Davis et al., 1996; Lane et al., 1996; Wang et al., 1998). Using the most 5′ cDNA as a probe to screen a mouse 129SvJ genomic library (Stratagene), we obtained one clone containing the second-fourth exons. A targeting construct was prepared by replacing the second exon containing the 5′ noncoding region, the ATG initiation codon and the signal sequence of Nr-CAM, with a neo cassette for positive selection. A thymidine kinase cassette was incorporated into the 3′ end of this clone for negative selection (both cassettes were gift of Dr. Yuji Mishina, NIEHS, Research Triangle Park, NC). The linearized construct was electroporated into W4 ES cell line established from 129SvEvS6/Taconic mice in the Transgenic Facility at NYU Medical Center (New York, NY) (Auerbach et al., 2000). Clones were selected using G418 and Gancyclovir and 11 clones out of 206 were shown to be positive for the targeting allele by Southern blotting analyses using both 5′ and 3′ probes. Three clones were chosen and morula aggregation was performed in the Transgenic Facility. Two clones were successfully transmitted into germline and two independent lines were established in both outbred (mixture of 129SvEvS6/Taconic and Swiss Webster) and 129SvEv inbred backgrounds. Both lines gave essentially the same results. Genotyping of mice was performed using either digoxigenin-based nonradioisotope Southern blotting (Roche) with a 3′ probe of EcoRV digested genomic DNA, or by PCR using specific primers sets to amplify the wild-type and neo allele.

General histology

Frozen sections from embryos and neonatal pups were prepared and immunohistochemistry was performed as described (Lustig et al., 2001). Antibodies used were 837/838, rabbit anti–Nr-CAM polyclonal antisera, (Lustig et al., 2001) 1:300; 371/372, rabbit anti-L1 polyclonal antisera (Lustig et al., 2001), 1:300; 4D7, mouse anti-TAG-1 monoclonal antibody (IgM, culture supernatant from Developmental Study Hybridoma Bank, University of Iowa, Iowa City, IA), 1:2; TG-3, rabbit anti-TAG-1 antisera (unpublished data), 1:1,000; rabbit anti-neurofascin polyclonal antisera (Tait et al., 2000), 1:1000; affinity-purified rabbit anti-contactin polyclonal antibody (gift of Dr. John Hemperly, Becton Dickinson Research Center, Research Triangle Park, NC) (Rios et al., 2000), 1:100; SMI31, mouse anti-neurofilament monoclonal antibody (Sternberger); 262, rabbit anti-Zic2 antisera, (gift of Dr. Steve Brown, Columbia University New York, NY) 1:10,000; and mouse anti-calbindin antibody (Sigma-Aldrich), 1:300. Secondary antibodies were from The Jackson Laboratory and used at 1:100–1:300. Adult mice were perfused transcardially with PBS followed by 4% paraformaldehyde and brains were dissected out and kept in 4% paraformaldehyde at 4°C overnight. Brains were embedded in 3% agarose and 100–150 mm vibratome sections were prepared. Immunostaining was performed with 2H3, mouse antineurofilament monoclonal antibody (culture supernatant from Developmental Study Hybridoma Bank) followed by HRP conjugated anti–mouse antibody with DAB as a substrate. Some frozen sections and vibratome sections were stained with cresyl violet, washed with water, and mounted on the Superfrost slide (Fisher Scientific) with gel mount (Biomeda) or Permount. Slides were observed under a Zeiss Axiophot microscope. Photographs were taken using either Kodak Ektachrome 400 (for fluorescence) or Kodak 64T (for bright field). In some cases, images were captured by CCD camera with AG-5 image grabber or Spot camera on a Nikon Diaphot microscope using NIH image software or Adobe PhotoShop software.

Analysis of cerebellar size of adult Nr-CAM knockout mice

Three pairs of 3–6-mo-old Nr-CAM −/− and their littermate Nr-CAM +/− (129SvEv genetic background) females were used for analysis of cerebellar size. First, brains were observed under the dissecting microscope and images were collected through CCD camera. Because we noticed a size difference in lobe IV+V at the midline, we cut brains sagittally at the midline and cut 100 μm vibratome sections starting from the midline. The images of the first two sections as floating sections were captured through CCD camera on a Nikon Diaphot microscope using a 2× objective. The area of gray matter corresponding to molecular layer and granule cell layer was easily visualized and was measured using NIH image software. The sections were further processed for Nissl staining and photographs were taken. To analyze midline sections by another method, we also performed the analysis by cutting brains sagittally at the left lateral edge of the brain and used this plane as a base for vibratome sectioning starting from the right edge of the brains. All sections were collected and, based on landmarks in cortical regions, including the presence of corpus callosum and absence of cross sections of cortical lobes, sections through the midline were identified. One section through the midline and one before and one after the midline sections were analyzed as above.

In situ hybridization

In situ hybridization was performed on vibratome sections using Nr-CAM specific probe as described (Lustig et al., 2001). In some cases, sections were further processed for immunostaining with anti-calbindin or anti-Zic2 antibody followed by HRP conjugated secondary antibody with DAB as a substrate. For calbindin staining, sections were treated with trypsin following manufactures protocol. Sections were mounted with gel mount or Permount and images were collected as above.

Neurite outgrowth assay

Contactin-Fc, βCFS-Fc (RPTPβ containing the extracellular C, F, and S domains), and Ng-CAM substrates were as described (Sakurai et al., 1997). Anti–Nr-CAM antibody was described previously (Lustig et al., 2001) and Fab′ fragments of anti–Nr-CAM antibody were prepared as described (Sakurai et al., 1997). Neurite outgrowth assay was performed as described (Sakurai et al., 1997) with slight modification to the media. In brief, substrates were spotted in a circular array in 35-mm petri dishes for 1 h at room temperature, followed by blocking with 1% BSA/PBS. Dissociated cells from P8 mouse cerebella were prepared and 250 μl of 2×10^5 cells/ml in Neurobasal media supplemented with B27 (GIBCO BRL) were plated. Cultures were incubated at 37°C for 24 h and fixed with 4% paraformaldehyde. Neurite outgrowth measurement was performed as described (Sakurai et al., 1997).

Biochemical procedure

Brains or cerebella from P8 pups were dissected out and extracted with extraction buffer containing 1% Triton X-100 using a glass Dounce homogenizer (Wheaton, A pastel, twenty strokes) as described (Sakurai et al., 1996). After clarification by centrifugation, extracts (100 μg) were incubated with the protein A beads (6.7 μl of a 50% slurry; Pierce Chemical Co.) that had been preincubated at 4°C overnight with culture supernatants (1.7 ml containing 1–2 μg/ml Fc fusion protein) from stable transfectants of 293 cells producing βC–Fc (RPTPβ containing the C domains) (Peles et al., 1995). Beads were washed with extraction buffer, and then SDS sample buffer was added and samples were separated on 7% SDS PAGE. Brain extracts from adult mice were prepared in the same way and 20 μg of extract was subjected to 7% SDS-PAGE. Western blotting was performed as described using ECL detection system (NEN Life Science Products) (Sakurai et al., 1996); primary antibodies used were 837 (1:300), 371 (1:500), anti-neurofascin (1:1,000) and anti-contactin (1:500).

Generation and analysis of Nr-CAM/L1 double knockout mice

L1 knockout mice were obtained from Dr. Bruce Trapp in the Cleveland Clinic Foundation, that were originally established and analyzed by Dr. P. Soriano and Dr. A. Furley (Cohen et al., 1998). These mice were kept in 129Sv genetic background. Because the L1 gene is on the X chromosome and male hemizygotes for the L1 mutation are effectively sterile, female heterozygotes for L1 mutation were crossed with Nr-CAM knockout males and female heterozygotes for L1 and Nr-CAM mutations were obtained. They were then crossed with Nr-CAM–null males. Because outbred mice yielded bigger litter size, we used outbred lines (mixture of 129SvEvS6/Taconic and Swiss Webster from Taconic) for these matings. Progeny from these matings were genotyped routinely at 3 wk. Genomic Southern blotting was performed sequentially on EcoRV digested DNA using the Nr-CAM 3′ probe and an L1 probe (Cohen et al., 1998).

Because there was a high incidence of death in these litters, brains were collected from pups when we noticed the presence of smaller pups in the litters at P3–P6 before they died ($n = 4$ at P3, $n = 4$ at P4, $n = 8$ at P5–P6). Randomly chosen littermates were also used for the analysis. Given the obvious size reduction of cerebella, we cut cerebella sagittally either by vibratome, cryosection or paraffin section, and midsagittal sections were analyzed. Brains were cut as frontal sections by vibratome, starting from the olfactory bulb and all sections were collected. The area of sagittally sectioned cerebella was measured using NIH image. For the brain size measurement, we picked two brain sections, which had corpus callosum, hippocampus, and the anterior edge of habenula and measured the area of frontally sectioned brain.

The thickness of EGL and IGL was measured on captured images of Nissl stained midsagittal sections of cerebellum using NIH image. The midpoint between posterior tip of lobe V and angle of fissure between lobe V and lobe VI was chosen to measure thickness of layers in lobe V. For lobe IX, the midpoint between the anterior tip and posterior tip of the lobe was chosen.

Mixed cerebellar cultures

Mixed cerebellar cultures were prepared from P0–P1 pups as described (Hatten et al., 1998) and plated on polylysine coated 16-well chamber slides. Antibodies were added at day 3 at 50 μg/ml, and media were changed every three days containing fresh antibodies. Cultures were fixed at d 6, 11, and 14 and stained with anti-α internexin, 1:300, a gift from Dr. Ron Liem (Columbia University, New York, NY) or anti-β-tubulin (Sigma-Aldrich; 1:1,000) antibodies followed by appropriate secondary antibodies and photographs were taken. Hoechst 33258 was added to the mounting media. Two fields were randomly chosen under 10× objectives using CCD camera and Hoechst 33258 positive nuclei were counted manually on captured images.

We thank Dr. Yuji Mishina for cassettes and advice for targeting construct; Dr. Alex Joyner and Ms. Anna Auerbach and their facilities for help with ES cell culture and morula aggregation; Drs. Phillipe Soriano, Bruce Trapp, and Carol Haney for supplying L1 knockout mice; Dr. Elior Peles for the reagents; Drs. John Hemperly and Ron Liem for anti-contactin and anti–α internexin, respectively; and Drs. Brent Kiernan, Heather Yeomans, Riva Marcus, Lynda Erskine, Rivka Rachel, Rich Blazeski, Janet Alder, George Zanazzi, and Evelyne Bloch-Gallego for stimulating discussion, comments, and technical help.

This work was supported by National Institutes of Health grant NS38949 to M. Grumet.

Submitted: 26 April 2001
Revised: 26 June 2001
Accepted: 2 August 2001

Note added in proof. Recent data on the genomic structure of human Nr-CAM (Dry, K., S. Kenwick, A. Rosenthal, and M. Platzer. 2001. *Gene*. 273: 115–122) suggests that the second exon in mouse corresponds to the fourth exon in human and other exons; numbers should be changed accordingly.

References

Alder, J., K.J. Lee, T.M. Jessell, and M.E. Hatten. 1999. Generation of cerebellar granule neurons in vivo by transplantation of BMP-treated neural progenitor cells. *Nat. Neurosci*. 2:535–540.

Aruga, J., T. Nagai, T. Tokuyama, Y. Hayashizaki, Y. Okazaki, V.M. Chapman, and K. Mikoshiba. 1996. The mouse zic gene family. Homologues of the *Drosophila* pair-rule gene odd-paired. *J. Biol. Chem*. 271:1043–1047.

Auerbach, W., J.H. Dunmore, V. Fairchild-Huntress, Q. Fang, A.B. Auerbach, D. Huszar, and A.L. Joyner. 2000. Establishment and chimera analysis of 129/SvEv- and C57BL/6-derived mouse embryonic stem cell lines. *Biotechniques*. 29:1024–1028; 1030; 1032.

Baptista, C.A., M.E. Hatten, R. Blazeski, and C.A. Mason. 1994. Cell-cell interactions influence survival and differentiation of purified Purkinje cells in vitro. *Neuron*. 12:243–260.

Berglund, E.O., K.K. Murai, B. Fredette, G. Sekerkova, B. Marturano, L. Weber, E. Mugnaini, and B. Ranscht. 1999. Ataxia and abnormal cerebellar microorganization in mice with ablated contactin gene expression. *Neuron*. 24: 739–750.

Brummendorf, T., and F.G. Rathjen. 1995. Cell adhesion molecules 1: immuno-

globulin superfamily. *Protein Profile*. 2:963–1008.

Buchstaller, A., S. Kunz, P. Berger, B. Kunz, U. Ziegler, C. Rader, and P. Sonderegger. 1996. Cell adhesion molecules NgCAM and axonin-1 form heterodimers in the neuronal membrane and cooperate in neurite outgrowth promotion. *J. Cell Biol*. 135:1593–1607.

Chen, S., N. Mantei, L. Dong, and M. Schachner. 1999. Prevention of neuronal cell death by neural adhesion molecules L1 and CHL1. *J. Neurobiol*. 38: 428–439.

Chien, C.L., C.A. Mason, and R.K. Liem. 1996. alpha-Internexin is the only neuronal intermediate filament expressed in developing cerebellar granule neurons. *J. Neurobiol*. 29:304–318.

Cohen, N.R., J.S. Taylor, L.B. Scott, R.W. Guillery, P. Soriano, and A.J. Furley. 1998. Errors in corticospinal axon guidance in mice lacking the neural cell adhesion molecule L1. *Curr. Biol*. 8:26–33.

Dahmane, N., and A. Ruiz-i-Altaba. 1999. Sonic hedgehog regulates the growth and patterning of the cerebellum. *Development*. 126:3089–3100.

Dahme, M., U. Bartsch, R. Martini, B. Anliker, M. Schachner, and N. Mantei. 1997. Disruption of the mouse L1 gene leads to malformations of the nervous system. *Nat. Genet*. 17:346–349.

Davis, J.Q., and V. Bennett. 1994. Ankyrin binding activity shared by the neurofascin/L1/NrCAM family of nervous system cell adhesion molecules. *J. Biol. Chem*. 269:27163–27166.

Davis, J.Q., S. Lambert, and V. Bennett. 1996. Molecular composition of the node of Ranvier: identification of ankyrin-binding cell adhesion molecules neurofascin (mucin+/third FNIII domain-) and NrCAM at nodal axon segments. *J. Cell Biol*. 135:1355–1367.

Demyanenko, G.P., A.Y. Tsai, and P.F. Maness. 1999. Abnormalities in neuronal process extension, hippocampal development, and the ventricular system of L1 knockout mice. *J. Neurosci*. 19:4907–4920.

Faivre-Sarrailh, C., J. Falk, E. Pollerberg, M. Schachner, and G. Rougon. 1999. NrCAM, cerebellar granule cell receptor for the neuronal adhesion molecule F3, displays an actin-dependent mobility in growth cones. *J. Cell Sci*. 112: 18:3015–3027.

Fransen, E., R. D'Hooge, G. Van Camp, M. Verhoye, J. Sijbers, E. Reyniers, P. Soriano, H. Kamiguchi, R. Willemsen, S.K. Koekkoek, C.I. De Zeeuw, P.P. De Deyn, A. Van der Linden, V. Lemmon, R.F. Kooy, and P.J. Willems. 1998. L1 knockout mice show dilated ventricles, vermis hypoplasia and impaired exploration patterns. *Hum. Mol. Genet*. 7:999–1009.

Garver, T.D., Q. Ren, S. Tuvia, and V. Bennett. 1997. Tyrosine phosphorylation at a site highly conserved in the L1 family of cell adhesion molecules abolishes ankyrin binding and increases lateral mobility of neurofascin. *J. Cell Biol*. 137:703–714.

Grumet, M. 1997. Nr-CAM: a cell adhesion molecule with ligand and receptor functions. *Cell Tissue Res*. 290:423–428.

Grumet, M., V. Mauro, M.P. Burgoon, G.M. Edelman, and B.A. Cunningham. 1991. Structure of a new nervous system glycoprotein, Nr-CAM, and its relationship to subgroups of neural cell adhesion molecules. *J. Cell Biol*. 113: 1399–1412.

Grumet, M., P. Milev, T. Sakurai, L. Karthikeyan, M. Bourdon, R.K. Margolis, and R.U. Margolis. 1994. Interactions with tenascin and differential effects on cell adhesion of neurocan and phosphacan, two major chondroitin sulfate proteoglycans of nervous tissue. *J. Biol. Chem*. 269:12142–12146.

Hatten, M.E., and N. Heintz. 1995. Mechanisms of neural patterning and specification in the developing cerebellum. *Annu. Rev. Neurosci*. 18:385–408.

Hatten, M.E., J. Alder, K. Zimmerman, and N. Heintz. 1997. Genes involved in cerebellar cell specification and differentiation. *Curr. Opin. Neurobiol*. 7:40–47.

Hatten, M.E., W.-Q. Gao, M.E. Morrison, and C.A. Mason. 1998. The cerebellum: purification and co-culture of identified cell populations. *In* Culturing Nerve Cells. G. Banker and K. Goslin, editors. MIT Press, Cambridge, MA. 419–459.

Hoffman, S., D.R. Friedlander, C.M. Chuong, M. Grumet, and G.M. Edelman. 1986. Differential contributions of Ng-CAM and N-CAM to cell adhesion in different neural regions. *J. Cell Biol*. 103:145–158.

Holm, J., R. Hillenbrand, V. Steuber, U. Bartsch, M. Moos, H. Lubbert, D. Montag, and M. Schachner. 1996. Structural features of a close homologue of L1 (CHL1) in the mouse: a new member of the L1 family of neural recognition molecules. *Eur. J. Neurosci*. 8:1613–1629.

Hortsch, M. 2000. Structural and functional evolution of the L1 family: are four adhesion molecules better than one? *Mol. Cell. Neurosci*. 15:1–10.

Kamiguchi, H., M.L. Hlavin, M. Yamasaki, and V. Lemmon. 1998. Adhesion molecules and inherited diseases of the human nervous system. *Annu. Rev. Neurosci*. 21:97–125.

Kayyem, J.F., J.M. Roman, E.J. de la Rosa, U. Schwarz, and W.J. Dreyer. 1992. Bravo/Nr-CAM is closely related to the cell adhesion molecules L1 and Ng-CAM and has a similar heterodimer structure. *J. Cell Biol*. 118:1259–1270.

Krushel, L.A., A.L. Prieto, B.A. Cunningham, and G.M. Edelman. 1993. Expression patterns of the cell adhesion molecule Nr-CAM during histogenesis of the chick nervous system. *Neuroscience*. 53:797–812.

Kuhar, S.G., L. Feng, S. Vidan, M.E. Hatten, and N. Heintz. 1993. Changing patterns of gene expression define four stages of cerebellar granule neuron differentiation. *Development*. 117:97–104.

Lagenaur, C., and V. Lemmon. 1987. An L1-like molecule, the 8D9 antigen, is a potent substrate for neurite extension. *Proc. Natl. Acad. Sci. USA*. 84:7753–7757.

Lane, R.P., X.N. Chen, K. Yamakawa, J. Vielmetter, J.R. Korenberg, and W.J. Dreyer. 1996. Characterization of a highly conserved human homolog to the chicken neural cell surface protein Bravo/Nr-CAM that maps to chromosome band 7q31. *Genomics*. 35:456–465.

Lindner, J., F.G. Rathjen, and M. Schachner. 1983. L1 Mono- and polyclonal antibodies modify cell-migration in early postnatal mouse cerebellum. *Nature*. 305:427–430.

Lustig, M., T. Sakurai, and M. Grumet. 1999. Nr-CAM promotes neurite outgrowth from peripheral ganglia by a mechanism involving axonin-1 as a neuronal receptor. *Dev. Biol*. 209:340–351.

Lustig, M., L. Erskine, C.A. Mason, M. Grumet, and T. Sakurai. 2001. Nr-CAM is expressed in the developing mouse nervous system: ventral midline structures, specific fiber tracts and neuropilar regions. *J. Comp. Neurol.* 433:13–28.

Mares, V., and Z. Lodin. 1970. The cellular kinetics of the developing mouse cerebellum. II. The function of the external granular layer in the process of gyrification. *Brain Res*. 23:343–352.

Mason, C.A., S. Christakos, and S.M. Catalano. 1990. Early climbing fiber interactions with Purkinje cells in the postnatal mouse cerebellum. *J. Comp. Neurol*. 297:77–90.

Morales, G., M. Hubert, T. Brummendorf, U. Treubert, A. Tarnok, U. Schwarz, and F.G. Rathjen. 1993. Induction of axonal growth by heterophilic interactions between the cell surface recognition proteins F11 and Nr-CAM/Bravo. *Neuron*. 11:1113–1122.

More, M.I., F.P. Kirsch, and F.G. Rathjen. 2001. Targeted ablation of NrCAM or ankyrin-B results in disorganized lens fibers leading to cataract formation. *J. Cell Biol*. 154:187–196.

Morrison, M.E., and C.A. Mason. 1998. Granule neuron regulation of Purkinje cell development: striking a balance between neurotrophin and glutamate signaling. *J. Neurosci*. 18:3563–3573.

Peles, E., M. Nativ, P.L. Campbell, T. Sakurai, R. Martinez, S. Lev, D.O. Clary, J. Schilling, G. Barnea, G.D. Plowman, et al. 1995. The carbonic anhydrase domain of receptor tyrosine phosphatase beta is a functional ligand for the axonal cell recognition molecule contactin. *Cell*. 82:251–260.

Rios, J.C., C.V. Melendez-Vasquez, S. Einheber, M. Lustig, M. Grumet, J. Hemperly, E. Peles, and J.L. Salzer. 2000. Contactin-associated protein (Caspr) and contactin form a complex that is targeted to the paranodal junctions during myelination. *J. Neurosci*. 20:8354–8364.

Rolf, B., M. Kutsche, and U. Bartsch. 2001. Severe hydrocephalus in L1-deficient mice. *Brain Res*. 891:247–252.

Sakurai, T., D.R. Friedlander, and M. Grumet. 1996. Expression of polypeptide variants of receptor-type protein tyrosine phosphatase beta: the secreted form, phosphacan, increases dramatically during embryonic development and modulates glial cell behavior in vitro. *J. Neurosci Res*. 43:694–706.

Sakurai, T., M. Lustig, M. Nativ, J.J. Hemperly, J. Schlessinger, E. Peles, and M. Grumet. 1997. Induction of neurite outgrowth through contactin and Nr-CAM by extracellular regions of glial receptor tyrosine phosphatase beta. *J. Cell Biol*. 136:907–918.

Schachner, M. 1997. Neural recognition molecules and synaptic plasticity. *Curr. Opin. Cell Biol*. 9:627–634.

Scotland, P., D. Zhou, H. Benveniste, and V. Bennett. 1998. Nervous system defects of ankyrinB (−/−) mice suggest functional overlap between the cell adhesion molecule L1 and 440-kD ankyrinB in premyelinated axons. *J. Cell Biol*. 143:1305–1315.

Stoeckli, E.T., and L.T. Landmesser. 1995. Axonin-1, Nr-CAM, and Ng-CAM play different roles in the in vivo guidance of chick commissural neurons. *Neuron*. 14:1165–1179.

Stoeckli, E.T., P. Sonderegger, G.E. Pollerberg, and L.T. Landmesser. 1997. Interference with axonin-1 and NrCAM interactions unmasks a floor-plate activity inhibitory for commissural axons. *Neuron*. 18:209–221.

Stottmann, R.W., and R.J. Rivas. 1998. Distribution of TAG-1 and synaptophysin

in the developing cerebellar cortex: relationship to Purkinje cell dendritic development. *J. Comp. Neurol*. 395:121–135.

Suter, D.M., G.E. Pollerberg, A. Buchstaller, R.J. Giger, W.J. Dreyer, and P. Sonderegger. 1995. Binding between the neural cell adhesion molecules axonin-1 and Nr- CAM/Bravo is involved in neuron-glia interaction. *J. Cell Biol*. 131: 1067–1081.

Tait, S., F. Gunn-Moore, J.M. Collinson, J. Huang, C. Lubetzki, L. Pedraza, D.L. Sherman, D.R. Colman, and P.J. Brophy. 2000. An oligodendrocyte cell adhesion molecule at the site of assembly of the paranodal axo-glial junction. *J. Cell Biol*. 150:657–666.

Tomoda, T., R.S. Bhatt, H. Kuroyanagi, T. Shirasawa, and M.E. Hatten. 1999. A mouse serine/threonine kinase homologous to *C. elegans* UNC51 functions in parallel fiber formation of cerebellar granule neurons. *Neuron*. 24:833–846.

Tuvia, S., T.D. Garver, and V. Bennett. 1997. The phosphorylation state of the FIGQY tyrosine of neurofascin determines ankyrin-binding activity and patterns of cell segregation. *Proc. Natl. Acad. Sci. USA*. 94:12957–12962.

Volkmer, H., R. Leuschner, U. Zacharias, and F.G. Rathjen. 1996. Neurofascin induces neurites by heterophilic interactions with axonal NrCAM while NrCAM requires F11 on the axonal surface to extend neurites. *J. Cell Biol*. 135: 1059–1069.

Wang, B., H. Williams, J.S. Du, J. Terrett, and S. Kenwrick. 1998. Alternative splicing of human NrCAM in neural and nonneural tissues. *Mol. Cell. Neurosci*. 10:287–295.

Yang, X.W., C. Wynder, M.L. Doughty, and N. Heintz. 1999. BAC-mediated gene-dosage analysis reveals a role for Zipro1 (Ru49/Zfp38) in progenitor cell proliferation in cerebellum and skin. *Nat. Genet*. 22:327–335.

Yoshihara, Y., M. Kawasaki, A. Tamada, S. Nagata, H. Kagamiyama, and K. Mori. 1995. Overlapping and differential expression of BIG-2, BIG-1, TAG-1, and F3: four members of an axon-associated cell adhesion molecule subgroup of the immunoglobulin superfamily. *J. Neurobiol*. 28:51–69.